Pergamon

J. Mech. Phys. Solids, Vol. 45, No. 7, pp. 1137–1159, 1997

0022–5096/97 $17.00 + 0.00

PII: S0022–5096(96)00122–6

NONLINEAR DELAMINATION MECHANICS FOR THIN FILMS

YUEGUANG WEI and JOHN W. HUTCHINSON

Division of Engineering and Applied Sciences, Harvard University, Cambridge, MA 02138, U.S.A.

(*Received* 5 *August* 1996; *in revised form* 8 *November* 1996)

ABSTRACT

Delamination of prestressed thin films on thick substrates is analysed accounting for plastic dissipation in either the substrate or film. Emphasis is on large scale yielding wherein the height of the plastic zone at the propagating interface crack tip is comparable to the film thickness. Such conditions are common for both metal and polymer thin films on elastic substrates or for ceramic coatings on metal substrates when the interface between the film and substrate is reasonably strong. Under large scale yielding, the notion of a thickness-independent interface toughness no longer pertains, and a nonlinear fracture mechanics is required to quantify delamination. Two such approaches are pursued in this paper using models based on the attainment of critical conditions at the interface crack tip within the plastic zone. Steady-state film delamination is analysed for conditions where yielding occurs either in the film or in the substrate, and critical combinations of prestress and thickness are predicted. The theory is applied to a recent set of experiments on copper films delaminating from silica substrates. © 1997 Elsevier Science Ltd

Keywords: A. crack tip plasticity, A. fracture toughness.

1. INTRODUCTION

A thin isotropic film of thickness h bonded to a thick substrate is subject to a uniform, equi-biaxial stress σ_R, as depicted for two types of problem in Fig. 1. The elastic energy per unit area in the bonded film is $(1-\nu)h\sigma_R^2/E$, where E and ν are the Young's modulus and Poisson's ratio of the film, respectively. When delamination occurs as a long interface crack releasing the elastic energy in the film without plastic deformation in the film, the energy release rate per unit of crack advance is

$$G = \frac{1-\nu^2}{2}\frac{h\sigma_R^2}{E}. \tag{1.1}$$

(The film is subject to the plane strain constraint in the x_3 direction leaving a residual stress $\sigma_{33} = (1-\nu)\sigma_R$ in the detached film.) For a perfectly brittle system, the critical condition for interface crack propagation is $G_{crit} = \Gamma_0$, where Γ_0 is the work per unit area of new surfaces consumed by the fracture process. Under steady-state propagation of the interface crack, the work rate balance under critical conditions for the case shown in Fig. 1(a) where *the film is elastic and the substrate elastic–plastic* is

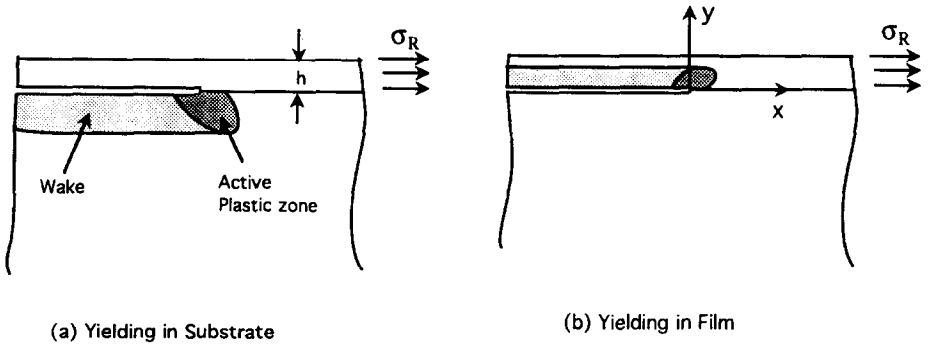

Fig. 1. Steady-state film delamination with plastic yielding: (a) in the substrate and (b) in the film.

$$G_{\text{crit}} = \Gamma_0 + \Gamma_P, \tag{1.2}$$

where Γ_0 is again the work per unit area consumed by the near-tip fracture process and Γ_P represents the sum of the plastic dissipation and the residual elastic energy stored in the remote wake. A precise definition of Γ_P is given in the Appendix. Equation (1.2) simply states that the elastic energy released by the film under steady-state propagation is dissipated in the work of the fracture process, in plasticity, and in any elastic energy remaining in the remote wake in the substrate. This energy balance neglects any frictional dissipation between the crack faces which will be in contact if $\sigma_R < 0$.

In the case where *the film is elasticplastic and the substrate is elastic*, (1.2) still applies in steady state, with G as the energy release rate determined from an elastic analysis, except that now Γ_P represents contributions from the plastic dissipation in the film induced by the propagating interface crack and any residual elastic energy left in the detached film. A precise definition of this term is also given in the Appendix.

The steady-state energy balance (1.2) for critical combinations of h and σ holds regardless of the vertical extent, H_P, of the active plastic zone of the propagating delamination crack. However, only if H_P is sufficiently small compared to the film thickness h will Γ_P be independent of h. In other words, the concept of a thickness-independent interface toughness, $\Gamma_i = \Gamma_0 + \Gamma_P$, as applied to thin film delamination requires that H_P be small compared to h, whether yielding occurs in the substrate or in the film itself. This is the relevant condition of small scale yielding for thin film delamination. More precisely, in small scale yielding, Γ_P may depend on the relative amount of mode II to mode I the interface experiences, but it will be independent of the film thickness. Only in small scale yielding can one speak of a steady-state interface toughness Γ_i which is unique to the interface (and mode mixity), and not dependent on extrinsic quantities such as the film thickness and the stress in the film. It will be seen, however, that in the limit of extremely thin films, plastic dissipation becomes a negligible fraction of Γ_0, even though H_P is comparable to h. In this limit, the notion of an interface toughness again applies but with $\Gamma_i = \Gamma_0$.

In this paper the mechanics of thin film delamination under general yielding conditions is addressed, where the plastic zone height is not necessarily small compared to the film thickness. Both tensile and compressive residual stress states will be

Table 1. *Representative plastic zone height estimates in small scale yielding*

	E (Gpa)	σ_Y (Mpa)	Γ_i (J m^{-2})	H_P (μm)
Polymer/metal or polymer/ceramic interface (polymer yields)	5	20	1	1.2
	5	20	50	62
	5	100	1	0.05
	5	100	50	2.5
Metal/ceramic interface (metal yields)	200	200	1	0.5
	200	200	100	50
	200	500	1	0.08
	200	500	100	8

considered. To reduce the number of parameters involved in the study, elastic mismatch between the film and the substrate will be ignored. Both are assumed to be isotropic, with E and ν as the common Young's modulus and Poisson's ratio, respectively. The tensile yield stress of the material that yields (either the film or the substrate, but not both) is denoted by σ_Y, with N as the strain hardening exponent.

To assess whether small scale yielding is likely to be applicable under a given set of circumstances, assume tentatively that it is and, for the purpose of comparison with the film thickness, use as the estimate of the associated plastic zone height:

$$H_P = \frac{1}{3\pi(1-\nu^2)} \frac{E\Gamma_i}{\sigma_Y^2}. \tag{1.3}$$

The parameters are those for the material undergoing plastic deformation. If small scale yielding really does apply and if Γ_i is the interface toughness, then (1.3) is the commonly used approximation for the height of a mode I plastic zone in plane strain. Values of H_P are given in Table 1 for representative interfaces, in each instance for a low toughness interface having little or no plastic dissipation ($\Gamma_i = 1$ J m^{-2}) and an interface of moderate toughness ($\Gamma_i = 50$ or 100 J m^{-2}). It is evident that many films whose thicknesses fall below 100 μm will be too thin for delamination to satisfy small scale yielding. In particular, only those film/substrate systems whose interface toughness is on the order of 1 J m^{-2} or smaller are likely to satisfy small scale yielding when the film thickness is on the order of 1 μm.

If small scale yielding applies, then (1.2) implies

$$(\sigma_R\sqrt{h})_{\text{critical}} = \left(\frac{2E\Gamma_i}{(1-\nu^2)}\right)^{1/2}. \tag{1.4}$$

where $\Gamma_i = \Gamma_0 + \Gamma_P$ is the mode-dependent, but thickness-independent, interface toughness. One objective of this paper is to obtain accurate estimates of the range of validity of (1.4) and to extend it into the range where small scale yielding does not apply. A more fundamental objective is to directly compute Γ_P in terms of the work of the fracture process Γ_0 and the other parameters characterizing the interface and the film/substrate system.

2. MODELS FOR NONLINEAR INTERFACE FRACTURE

Two models will be employed for the purpose just described: the embedded fracture process zone model of Needleman (1987) and Tvergaard and Hutchinson (1992, 1993), subsequently referred to as the EPZ model; and the plasticity-free strip model of Suo, Shih and Varias (1993), labeled the SSV model. When crack growth occurs in the presence of large scale yielding, it becomes essential to use a criterion based on critical values of near-tip deformation measures. In early work on crack growth, a criterion for continuing crack advance based on a critical near-tip opening angle or, equivalently, a critical near-tip crack opening profile, has been used. A similar criterion could be used here. Instead, we have preferred to invoke more mechanistically based models which, in principle, have greater potential of being tied directly to parameters of the fracture process.

The two models used here are indicated in Fig. 2 for the case where the film is elastic and the substrate is elastic–plastic. Plane strain conditions are assumed for both models. In each case, J_2 flow theory of plasticity is used to characterize deformation in the substrate. This theory is based on the von Mises, or J_2, yield surface. The small strain version of the theory is employed, consistent with the fact that the strains at the tip of the steadily growing crack are indeed small under conditions in which interface delamination occurs. The tensile stress–strain relation used in the present study is

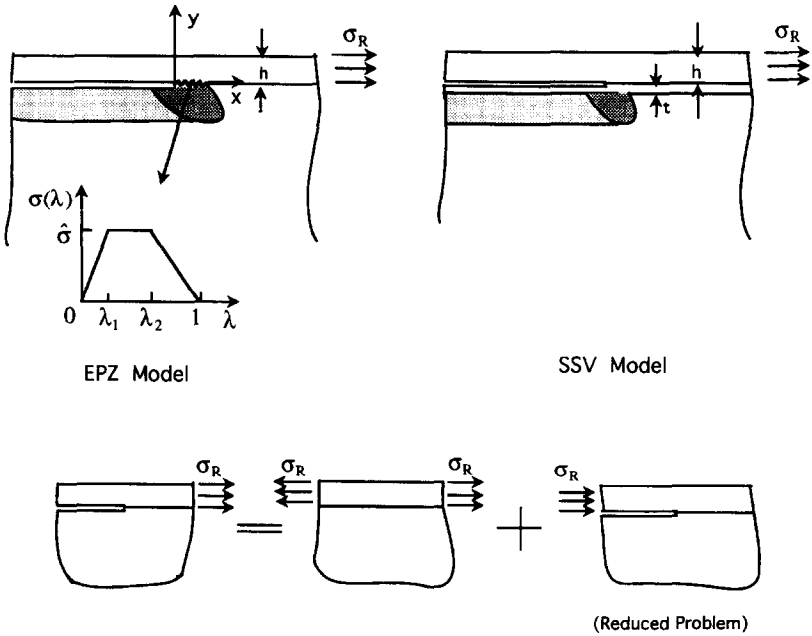

Fig. 2. Two models for thin film delamination for the case in which the substrate yields plastically: the embedded fracture process zone (EPZ) model and the Suo–Shih–Varias (SSV) model. The reduced problem employed in the numerical analysis is shown.

$$\varepsilon = \sigma/E \quad \text{for } \sigma \leqslant \sigma_Y$$
$$= (\sigma_Y/E)(\sigma/\sigma_Y)^{1/N} \quad \text{for } \sigma > \sigma_Y. \tag{2.1}$$

As already mentioned, the elastic properties of the film and the substrate are taken to be the same with Poisson's ratio ν chosen as 0.3 in all the calculations.

2.1. *The EPZ model*

In the EPZ model a traction–separation law characterizing the interface fracture process is embedded as a boundary condition along the interface. In the present applications of the model, the fracture process zone along the interface lies between the plastic zone on one side of the interface and elastic material on the other. Once the parameters of the fracture process separation law are specified, the model can be used to predict the relation between crack advance and applied stress. Under steady-state delamination, which will be the focus here, critical combinations of film thickness h and residual stress σ_R can be computed in terms of the properties of the film, substrate, and interface.

Following the notation for the law introduced in Tvergaard and Hutchinson (1993, 1994), let δ_n and δ_t be the normal and tangential components of the relative displacement of the crack faces across the interface in the zone where the fracture process occurs, as indicated in Fig. 2. Let δ_n^c and δ_t^c be critical values of these displacement components, and define a single dimensionless separation measure as

$$\lambda = \sqrt{(\delta_n/\delta_n^c)^2 + (\delta_t/\delta_t^c)^2} \tag{2.2}$$

such that the tractions drop to zero when $\lambda = 1$. With $\sigma(\lambda)$ displayed in Fig. 2, a potential from which the tractions are derived is defined as

$$\Phi(\delta_n, \delta_t) = \delta_n^c \int_0^\lambda \sigma(\lambda')\, d\lambda'. \tag{2.3}$$

The normal and tangential components of the traction acting on the interface in the fracture process zone are given by

$$T_n = \frac{\partial \Phi}{\partial \delta_n} = \frac{\sigma(\lambda)}{\lambda}\frac{\delta_n}{\delta_n^c}, \quad T_t = \frac{\partial \Phi}{\partial \delta_t} = \frac{\sigma(\lambda)}{\lambda}\frac{\delta_t}{\delta_t^c}\frac{\delta_n^c}{\delta_t^c}. \tag{2.4}$$

The traction law under a purely normal separation ($\delta_t = 0$) is $T_n = \sigma(\lambda)$ where $\lambda = \delta_n/\delta_n^c$. Under a purely tangential displacement ($\delta_n = 0$), $T_t = (\delta_n^c/\delta_t^c)\sigma(\lambda)$ where $\lambda = \delta_t/\delta_t^c$. The peak normal traction under purely normal separation is $\hat{\sigma}$, and the peak shear traction is $(\delta_n^c/\delta_t^c)\hat{\sigma}$ in a purely tangential 'separation'. The work of separation per unit area of interface Γ_0 is given by (2.3) with $\lambda = 1$. For the separation function $\sigma(\lambda)$ specified in Fig. 2,

$$\Gamma_0 = \tfrac{1}{2}\hat{\sigma}\delta_n^c[1 - \lambda_1 + \lambda_2]. \tag{2.5}$$

The parameters governing the separation law of the interface are the work of the fracture process Γ_0, the peak stress quantity $\hat{\sigma}$, and the critical displacement ratio δ_n^c/δ_t^c, together with the factors λ_1 and λ_2 governing the shape of the separation

function. Note that use of the potential ensures that the work of separation is Γ_0 regardless of the combination of normal and tangential displacements taking place in the process zone. Experience gained in the earlier studies suggests that the details of the shape of the separation law are relatively unimportant. The two most important parameters characterizing the fracture process in this model are Γ_0 and $\hat{\sigma}$. The parameter δ_n^c/δ_t^c is the next most important, but the study of mixed mode interface toughness using this model (Tvergaard and Hutchinson, 1993) indicates that predictions are relatively insensitive to this parameter for the mode combinations representative of film delamination. The one exception is the case where σ_R is compressive, which gives rise to delamination under mode II conditions. Then the peak in the shearing stress controls the fracture process, and the parameter δ_n^c/δ_t^c becomes important.

The condition for crack advance is attainment of $\lambda = 1$ at the current end of the traction–separation zone. In steady-state propagation, this condition must be imposed on the solution, as will be discussed further below.

2.2. *The SSV model*

One limitation of the EPZ model as specified above is its failure to provide realistic predictions when the peak interface separation stress $\hat{\sigma}$ is prescribed to be at levels thought to be required for separation of strong interfaces at the atomic level, as will be evident from the numerical results described subsequently. This limitation appears to be primarily a consequence of the inadequacy of conventional plasticity to account for stress elevation in the region of high strain gradients at the tip of the crack. The limitations of the EPZ model will be further discussed in Section 5. At this point, however, they serve to motivate the rationale for the SSV model. Under the assumption that dislocations emitted at the crack tip play a minimal role in crack propagation for the class of interfaces under study, Suo *et al.* (1993) proposed a model capable of producing the high stresses at the crack tip necessary for atomic separation. They imposed an elastic, plasticity-free strip between the line of the crack and the plastic zone. For the case in which the substrate is elastic–plastic, a strip of thickness t with the same elastic properties as the substrate is inserted below the interface, as shown in Fig. 2. When there is no elastic mismatch between the film and substrate, the interface crack tip lies within an elastically homogeneous region. It therefore has the conventional $1/\sqrt{x_1}$ stress singularity with stress intensities K_I^{tip} and K_{II}^{tip} and near-tip energy release rate $G_{tip} = (1-\nu^2)(K_I^{tip^2} + K_{II}^{tip^2})/E$. According to the model, crack propagation requires $G_{tip} = \Gamma_0$, the work of the fracture process. Thus, the computation problem for the SSV model involves computation of G_{tip} in terms of the properties of the film and the substrate and h and σ, with the imposition of $G_{tip} = \Gamma_0$ to obtain propagation conditions. Beltz *et al.* (1996) have suggested a self-consistent procedure for estimating the thickness t of the plasticity-free strip, but here t will be regarded as a free "material" parameter in the model. Diminishing t has an effect similar to that of increasing $\hat{\sigma}$ in the EPZ model, as will be illustrated below.

2.3. *Computational method for steady-state delamination*

The cartoon in the lower part of Fig. 2 indicates that the problem for a semi-infinite interface crack propagating under steady-state conditions can be decomposed into a

sum of the initial state plus a reduced problem. The figure is drawn to illustrate the situation for a residual biaxial tensile stress σ_R in the film. Superposition holds even though the problem is nonlinear because the stress in the substrate is zero in the absence of the crack. For the problems in which plasticity occurs in the film, the same decomposition can be used but it then becomes necessary to account for the initial stress state σ_R in the yield condition of the reduced problem. In both cases, the reduced problem supplies the results needed to predict steady-state delamination.

In steady-state, an observer translating with the tip of the crack sees unchanging stress and strain fields. A zone of active plasticity moves with the tip leaving behind a wake of plastically deformed material within which elastic unloading has occurred. A residual stress distribution $\sigma_{11}(x_2)$, together with $\sigma_{33}(x_2)$, will generally exist in the remote wake. Under steady-state, the condition for any quantity such as a Cartesian component of the plastic strain rate is

$$\dot{\varepsilon}_{ij}^{P} = -\dot{a}\frac{\partial \varepsilon_{ij}^{P}}{\partial x_1}, \tag{2.6}$$

where the crack is advancing in the x_1 direction and $\dot{a}$ is the rate of its advance. The material point currently at (x_1, x_2) has experienced the deformation history of the spatial sequence of material points upstream along (∞, x_2). Thus, the steady-state problem can be posed in a way that bypasses the necessity to solve the transient history building up to steady state. An iterative numerical method (Dean and Hutchinson, 1980) is used to obtain the steady-state solution. A similar method was employed by Suo *et al.* (1993) and Beltz *et al.* (1996). A finite element procedure is used with a grid designed to cope with the required integrations from far upstream along lines parallel to the x_1 axis.

3. ELASTIC FILM AND ELASTIC–PLASTIC SUBSTRATE

3.1. *The EPZ model*

There is only one material-based length parameter in the problem. Following Tvergaard and Hutchinson (1992, 1993), we chose that parameter to be

$$R_0 = \frac{1}{3\pi(1-\nu^2)}\frac{E\Gamma_0}{\sigma_Y^2}. \tag{3.1}$$

This reference length is an estimate of the height of the plastic zone in the substrate assuming the interface crack is loaded by an applied mode I stress intensity $K_I = \sqrt{E\Gamma_0/(1-\nu^2)}$. In other words, R_0 can be regarded as an estimate of the plastic zone height in mode I in the limit where plastic dissipation is small. Dimensional analysis dictates that the critical value of σ_R can be expressed as a function of the dimensionless parameters:

$$\left(\frac{\sqrt{h}\sigma_R}{\sqrt{E\Gamma_0}}\right)_{crit} = f\left[\frac{h}{R_0}, \frac{\hat{\sigma}}{\sigma_Y}, N, \frac{\sigma_Y}{E}, \nu\right]. \tag{3.2}$$

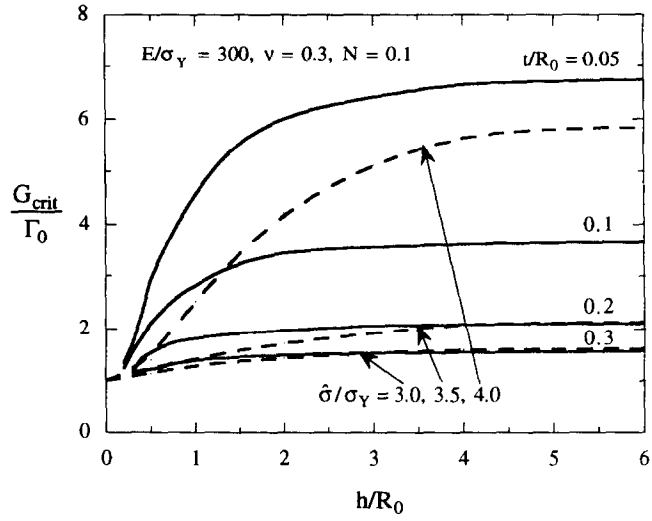

Fig. 3. Critical value of G as a function of film thickness when substrate yields. Solid line curves apply to SSV model and dashed line curves to EPZ model. For $\sigma_R > 0$.

It is more insightful to retain G as defined as (1.1) as a variable in the solution; thus an equivalent form of (3.2) is used:

$$\frac{G_{\text{crit}}}{\Gamma_0} = F\left[\frac{h}{R_0}, \frac{\hat{\sigma}}{\sigma_Y}, N, \frac{\sigma_Y}{E}, \nu\right]. \tag{3.3}$$

Not explicitly indicated is an additional dependence on the sign of the prestress σ_R. Numerical calculations carried out with various values of σ_Y/E and ν reveal that these parameters of the set in (3.3) have only a minor influence on G_{crit}/Γ_0. The other dimensionless parameters strongly affect the solution. Plots of G_{crit}/Γ_0 as a function of the normalized film thickness are included in Fig. 3 for $\sigma_R > 0$ for three values of $\hat{\sigma}/\sigma_Y$ with $N = 0.1$, $\sigma_Y/E = 1/300$ and $\nu = 0.3$. The asymptote to any of these curves as h/R_0 increases corresponds to the small scale yielding limit with $G_{\text{crit}}/\Gamma_0 \to \Gamma_i/\Gamma_0$. In the limit when h/R_0 becomes small, plastic dissipation Γ_P becomes a small fraction of Γ_0 and $G_{\text{crit}}/\Gamma_0 \to 1$, even though the plastic zone height becomes greater than the film thickness (as can be seen below in Fig. 6). Large scale yielding effects dominate in the transition from small scale yielding to the limit of small h/R_0, roughly corresponding to h/R_0 in the range from about 0.5 to 5, with some dependence on $\hat{\sigma}/\sigma_Y$.

The effect of large scale yielding on the relationship between the critical delamination stress and film thickness can be seen in Fig. 4, where the results from Fig. 3 are replotted as $(\sigma_R\sqrt{h})_{\text{crit}}/\sqrt{2E\Gamma_i/(1-\nu^2)}$ versus h/R_0. As discussed above, Γ_i is the interface toughness under small scale yielding conditions (i.e. the limit of G_{crit} as h/R_0 becomes large). In this form, the range of h/R_0 over which small scale yielding limit (1.4) holds is evident, as is the reduction of $(\sigma_R\sqrt{h})_{\text{crit}}$ when large scale yielding takes effect. When h/R_0 approaches zero, it has been noted that G_{crit} approaches Γ_0. In Fig. 4, this limit corresponds to the ordinate intercept $\sqrt{\Gamma_0/\Gamma_i}$. Figure 4 clearly reveals the transition from small scale yielding to the limit of very thin films, where plastic

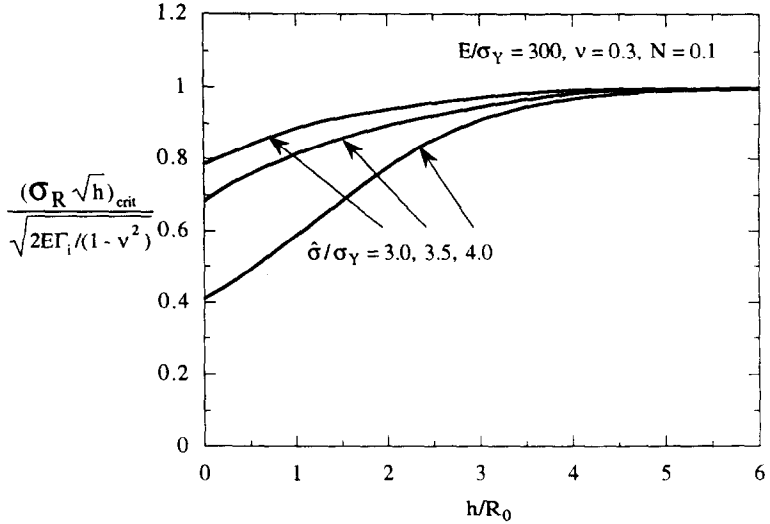

Fig. 4. Critical combination of $\sigma\sqrt{h}$ as a function of film thickness for yielding in the substrate according to the EPZ model. For $h/R_0 > 5$, the critical combination for delamination becomes independent of film thickness. The interface toughness Γ_i applies for "thick" films in this range. For $\sigma_R > 0$.

dissipation in the substrate makes a negligible contribution to the delamination energy. In summary: *when the film thickness is smaller than that required for small scale yielding, the critical delamination stress can be significantly below a prediction based on* (1.4) *using an interface toughness* Γ_i *obtained from a "thick" film test. Moreover, when the film is sufficiently thin,* G_{crit} *approaches* Γ_0.

3.2. *The SSV model*

There are two material-based length quantities in the SSV model of the elastic film on the elastic–plastic substrate: R_0 and t. For this model, dimensional analysis gives

$$\frac{G_{crit}}{\Gamma_0} = F\left[\frac{h}{R_0}, \frac{t}{R_0}, N, \frac{\sigma_Y}{E}, \nu\right]. \tag{3.4}$$

The measure of the near-tip combination of modes, $\Psi_{tip} = \tan^{-1}(K_{II}^{tip}/K_I^{tip})$, depends on the same dimensionless parameter set. Curves of G_{crit}/Γ_0 versus h/R_0 computed for this model for $\sigma_R > 0$ are also shown in Fig. 3, in this case for four values of t/R_0 but otherwise for the same parameters as chosen for the EPZ model. The trends are similar as those for the EPZ model, and it is clear that the parameter t/R_0 characterizing the thickness of the plasticity-free zone plays a role similar to that of $\hat{\sigma}/\sigma_Y$ in that model. The SSV model predicts that the transition to large scale yielding occurs at a slightly smaller film thickness than that predicted by the EPZ model.

A selection of plastic zone shapes is plotted in Fig. 5. Only the active portion of the zone is shown, as the unloading wake is omitted for clarity. The zones in Fig. 5 are all for $h/R_0 = 6$, corresponding to systems well into the small scale yielding range. Differing scales are used in the horizontal and vertical directions. The remarkable feature of these results is the extent of the active plastic zone ahead of the tip in the

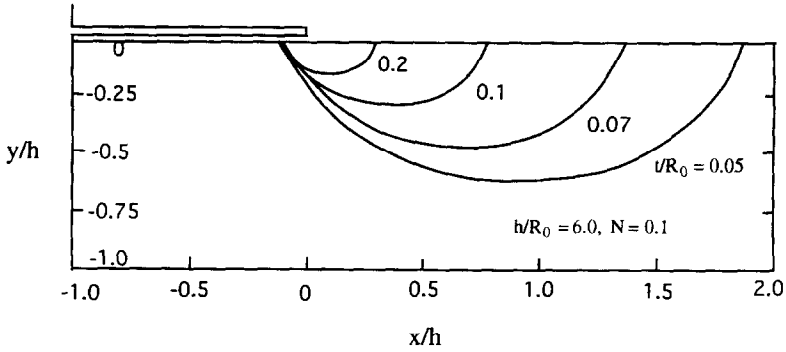

Fig. 5. Active plastic zones for the SSV model in the small scale yielding ($E/\sigma_Y = 300$, $\nu = 0.3$).

substrate. For example, for $t/R_0 = 0.05$, the plastic zone extends ahead of the crack tip by almost twice the film thickness and extends below the interface to a depth of about two thirds of the film thickness. Nevertheless, small scale yielding holds in the sense that G_{crit} is independent of h, as is evident from Fig. 3. Other crack problems are known such that small scale yielding prevails when the plastic zone is much larger than one might expect based on the simplest notion of the zone of dominance of the elastic K-field. The present thin film problem seems truly exceptional in this respect. The implication of these results is that thickness-independent interface toughness, Γ_i, holds to much smaller film thicknesses than one might expect on the basis of simple comparative estimates such as those made in the Introduction.

The second set of active plastic zone plots in Fig. 6 are all computed with the same normalized thickness of the plasticity-free strip, $t/R_0 = 0.1$, but with values of the normalized film thickness, h/R_0, ranging from small scale yielding to large scale yielding. Two normalizations of the coordinates are used to reveal different aspects of yield behavior. In Fig. 6(a) the coordinates are again normalized by the film thickness h, but in Fig. 6(b) the same zone shapes are presented using coordinates normalized by R_0. The zones in Fig. 6(a) show, indeed, for $h/R_0 < 1$, that the zone extends to depths below the interface of more than several times h. Consistent with the expectation from large scale yielding, a thickness-independent interface toughness no longer pertains. On the other hand, the coordinate normalizations used in Fig. 6(b) show that the absolute size of the plastic zone diminishes as h decreases. This is consistent with the trend seen in Fig. 3 where plastic dissipation becomes negligible and G_{crit} decreases to Γ_0 as h/R_0 becomes small. Moreover, the plots in Fig. 6(b) reveal that the absolute size of the plastic zone becomes essentially independent of the film thickness for h/R_0 greater than about 3, in accordance with the fact that a thickness-independent interface toughness governs in this regime.

Companion plots to those in Fig. 3 for the SSV model are given for Ψ_{tip} in Fig. 7. For reference, it can be noted that $\Psi_{tip} = 52.1^\circ$ when the problem is strictly elastic with no mismatch in properties across the interface (Hutchinson and Suo, 1992). For $h/R_0 > 2$, the values of Ψ_{tip} in Fig. 7 are different from 52.1° owing to the existence of the plastic zone separating the plasticity-free strip from the outer elastic region. The numerical results suggest that Ψ_{tip} approaches the elastic mode mixity, 52.1°, as h/R_0 becomes small. This is not entirely surprising in light of the fact that plastic dissipation

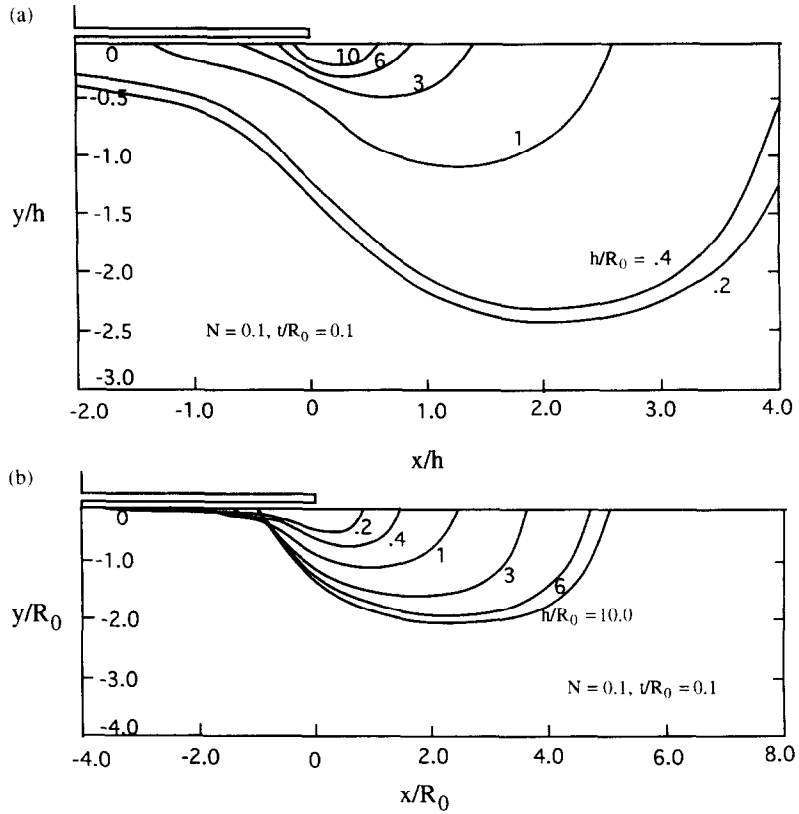

Fig. 6. Active plastic zones for the SSV model for $t/R_0 = 0.1$ and various film thicknesses: (a) relative to the film thickness h and (b) relative to the material length scale R_0.

becomes negligible compared to Γ_0 in this limit. However, it does run counter to what one would expect, given that the size of the plastic zone becomes large compared to the film thickness in this limit.

Other trends computed using the SSV model are displayed in Fig. 8. Variations of G_{crit}/Γ_0 as a function of t/R_0 are plotted in Fig. 8(a) for three values of the strain hardening exponent and two values of the normalized film thickness, both of which fall within, or nearly within, the small scale yielding range. The effect of strain hardening is significant: the contribution to interface toughness from plastic dissipation from a high hardening substrate is much less than that from a low hardening substrate. The effect of the sign of the residual stress in the film is illustrated in Fig. 8(b), where curves for compressive σ_R can be compared with curves calculated for tensile σ_R, with all other parameters taken to be identical. According to the SSV model, there is almost no difference in the values of G_{crit}/Γ_0 in the two cases even though the film with $\sigma_R < 0$ delaminates as a closed mode II crack. It must be emphasized, however, that frictional dissipation due to sliding contact of the crack faces has been ignored. It should also be noted that there is likely to be more of a difference between the tensile and compressive cases according to the EPZ model, with sensitivity to the parameter ratio δ_n^c/δ_t^c.

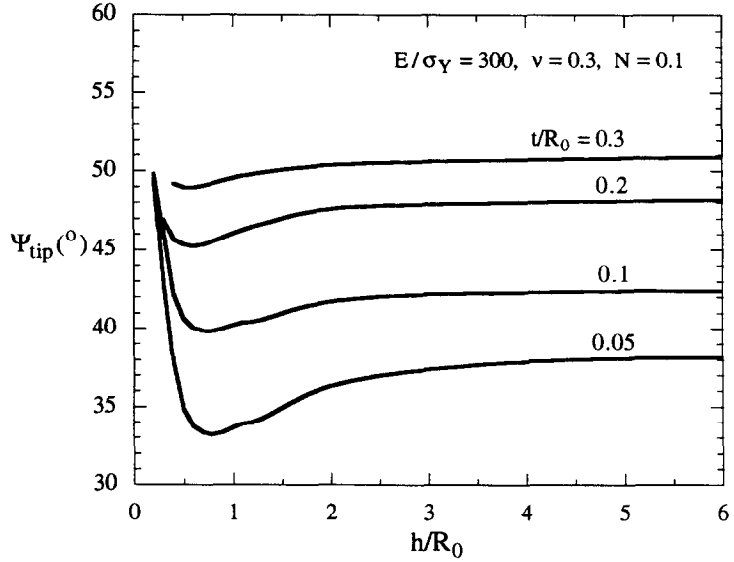

Fig. 7. Mode mixity at tip within the elastic strip for the SSV model results in Fig. 3.

4. ELASTIC–PLASTIC FILM AND ELASTIC SUBSTRATE

In this section, metal or polymer films bonded to elastic substrates are considered. Attention is restricted to films under equi-biaxial tension σ_R which are *at yield*. Such conditions are common for films that are bonded or deposited to a substrate at an elevated temperature and then cooled. Films can also be brought to yield if the substrate is deformed. Thus, for all the cases considered in this section, we take σ_Y to be the current yield stress in the attached film and employ the stress–strain relation (2.1) to apply to subsequent deformations in the incremental constitutive law. The collection of terms defining G in (1.1) remains in effect. As a result of $\sigma_R = \sigma_Y$, the film stress is no longer an independent variable, and the issue of large versus small scale yielding is moot. The number of variables is reduced by one with consequences for the dimensionless form of the solution. Specifically, with $\sigma_R = \sigma_Y$, $G/\Gamma_0 = (1/6\pi)h/R_0$, such that h/R_0 is no longer an independent parameter in the set of variables in (3.3) and (3.4). For the EPZ model, the dimensionless form of the solution reduces to

$$\frac{G_{\text{crit}}}{\Gamma_0} = F\left[\frac{\hat{\sigma}}{\sigma_Y}, N, \frac{\sigma_Y}{E}, \nu\right], \tag{4.1}$$

while for the SSV model it is

$$\frac{G_{\text{crit}}}{\Gamma_0} = F\left[\frac{t}{R_0}, N, \frac{\sigma_Y}{E}, \nu\right]. \tag{4.2}$$

The reference length R_0 is still defined by (3.1), but now with σ_Y representing the properties of the film. It should be noted that G as defined here corresponds to the

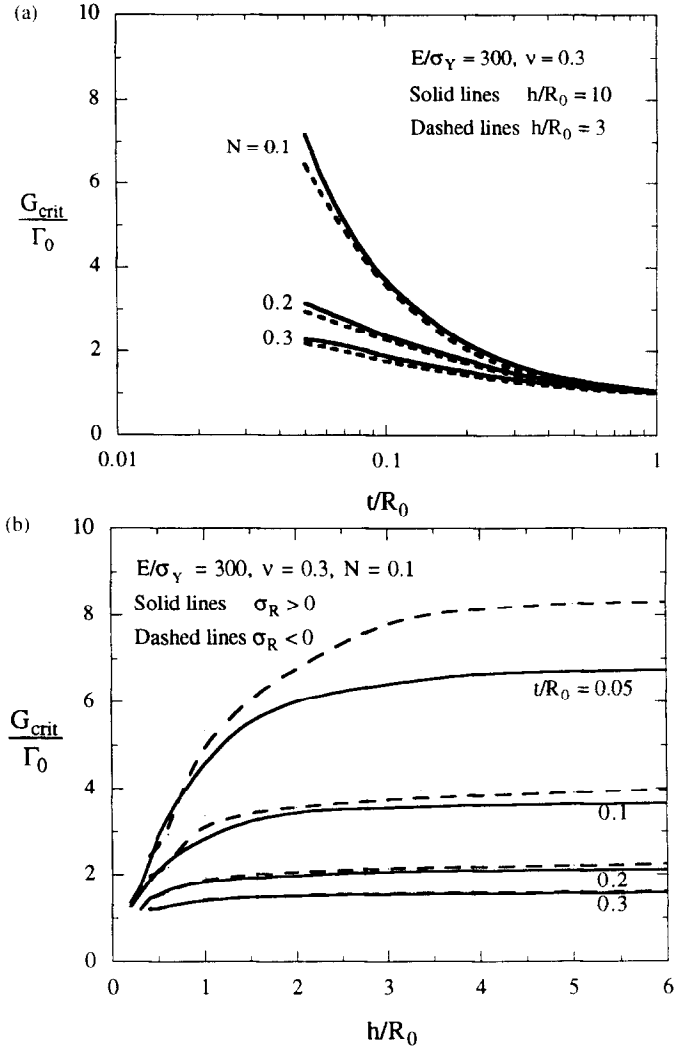

Fig. 8. Trends predicted by the SSV model. (a) With t/R_0 for three strain hardening levels and two values of h/R_0; (b) with h/R_0 for three values of t/R_0 and comparing predictions for films with a compressive prestress to those for films with a tensile prestress.

energy release rate assuming the film undergoes only elastic unloading, while, in fact, reversed plasticity in the vicinity of the interface crack does occur. Nevertheless, as mentioned in the Introduction, it is insightful to retain G as the collection of variables in (1.1). The form of the solution (4.2) is rigorous. Further discussion of the steady-state energy balance is given in the Appendix.

The essence of interface delamination when the attached film is at yield is the release of stress producing elastic unloading except in an active plastic zone at the crack tip. Attainment of the critical delamination condition, $G = G_{crit}$, can be achieved either by reaching a sufficiently high stress, as might occur by an imposed temperature

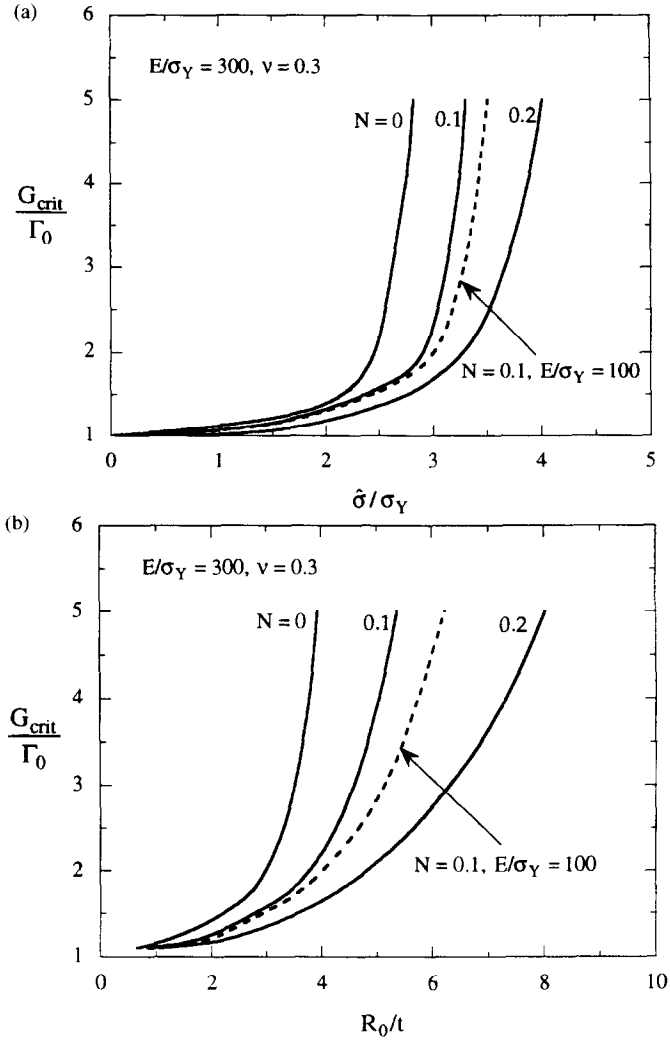

Fig. 9. Critical values of G for films that yield plastically where the tensile stress in the film is at yield prior to delamination. (a) EPZ model; (b) SSV model.

reduction on the film/substrate system, or by reaching a critical thickness in instances where films are deposited under conditions giving rise to intrinsic tensile stresses. Plots of G_{crit}/Γ_0 as a function of $\hat{\sigma}/\sigma_Y$ for three levels of strain hardening are presented in Fig. 9(a) for the EPZ model. Corresponding plots for the SSV model are given in Fig. 9(b) with R_0/t as the interface parameter. The other interface parameters for the EPZ model have been chosen to be identical to those used in Section 3. The effect of varying σ_Y/E, independently of the other dimensionless parameters in (4.1) and (4.2), is seen to be fairly small for each of the models in Fig. 9. The two parts of Fig. 9 emphasize the qualitative similarity in the two models noted earlier, with $\hat{\sigma}/\sigma_Y$ in the EPZ model playing a role similar to R_0/t in the SSV model. When either of these

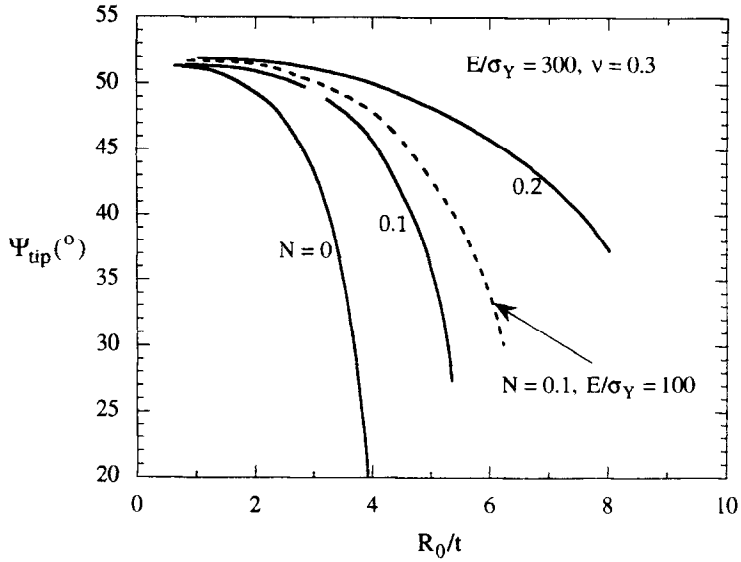

Fig. 10. Mode mixity at tip within the elastic strip for the SSV model results in Fig. 9(b).

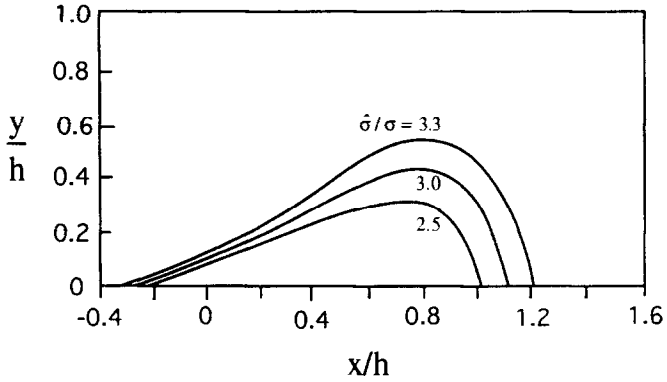

Fig. 11. Active plastic zones in the film for the EPZ model.

parameters is larger than about 2 or 3, depending on N, plastic dissipation makes a significant contribution to delamination with G_{crit}/Γ_0 increasing sharply as these interface parameters increase. The measure of near-tip mode combination, Ψ_{tip}, associated with the SSV model predictions in Fig. 9(b) is plotted in Fig. 10. It can be seen that the elastic mode mix for this configuration, 52.1°, is approached for small R_0/t, while near-tip conditions become increasing dominated by mode I when plastic dissipation becomes significant. A similar effect is observed for the EPZ model, namely normal separations increasingly dominate the fracture process zone as $\hat{\sigma}/\sigma_Y$ increases even though the elastic problem has roughly equal amounts of modes I and II. Active plastic zones for the EPZ model are displayed in Fig. 11.

5. AN APPLICATION: THIN COPPER FILMS ON SILICA SUBSTRATES

Polycrystalline copper films have been vapor deposited or diffusion bonded to silica substrates at thicknesses ranging from less than 0.1 μm to almost 100 μm and tested to determine conditions for delamination (Bagchi *et al.* 1994; Bagchi and Evans, 1996). The films are at yield at the test temperature (20°C), and the strong dependence of σ_Y on film thickness h [Fig. 12(a)] is typical for very thin metal films (Nix, 1989; Vinci *et al.*, 1995). The stress in the copper film by itself does not lead to delamination. Delamination was achieved with the aid of a technique developed by Bagchi and Evans, wherein a film of chromium was vapor deposited on top of the copper. The Cr film bonds well to the copper and deposits with a high residual tension. By systematically increasing the thickness of the Cr film, the critical condition is reached such that the combined elastic energy stored in the two-layer film is sufficient to delaminate the copper/SiO_2 interface. It is believed that the Cr layer does not experience plastic deformation. In the notation of the present paper, the experimental data points in Fig. 12(b) are shown as G_{crit} versus copper film thickness h_{cu}, where G is the energy release rate computed on the basis of a steady-state *elastic analysis* of the two-layer film.

To apply the theoretical delamination results of Section 4 to this system, express the dependence of σ_Y on the copper film thickness as

$$\sigma_Y = \sigma_Y^0[1+\sqrt{(h_0/h_{cu})}] \tag{5.1}$$

where plots for two choices of pairs (σ_Y^0, h_0) are included in Fig. 12(a). it will be assumed that (5.1) applies to the diffusion bonded films as well as the vapor deposited films, although yield data on the thicker diffusion bonded films were not obtained. Since the copper film is at yield, the dependence of G_{crit} on the thickness of the copper film according to the EPZ model follows by combining (5.1) with (4.1) to give

$$\frac{G_{crit}}{\Gamma_0} = F\left[\frac{\hat{\sigma}}{\sigma_Y^0[1+\sqrt{(h_0/h_{cu})}]}, N, \frac{\sigma_Y}{E}, \nu\right]. \tag{5.2}$$

This result can only be regarded as an approximation in the present application since details associated with the two-layered film are not fully taken into account. Plastic deformation in the copper will effect the energy released by the Cr layer. moreover, even though the Cr layer does not deform plastically, it may have some effect on the plastic dissipation in the copper. A more accurate analysis will require computations to be carried out specifically for the two-layer film system. Nevertheless, it is expected that (5.2) should supply a reasonably good approximation for the EPZ model in this application.

Plots of G_{crit} versus h_{cu} from (5.2) are included in Fig. 12(b) for each of the two choices of (σ_Y^0, h_0) with $\Gamma_0 = 0.7$ J m^{-2}, and with three choices for $\hat{\sigma}$ (i.e. 1, 1.5, and 2 GPa). The theoretical plots are made with $N = 0.1$ and $\nu = 0.3$. The thickness dependence of the third dimensionless variable in (5.2), σ_Y/E, could be taken into account with additional calculations but was ignored because of its secondary importance; $\sigma_Y/E = 1/300$ was used. Thus, all the theoretical curves in Fig. 12(b) are obtained from the curve for $N = 0.1$ and $\sigma_Y/E = 1/300$ in Fig. 9(a). Since the copper film is at

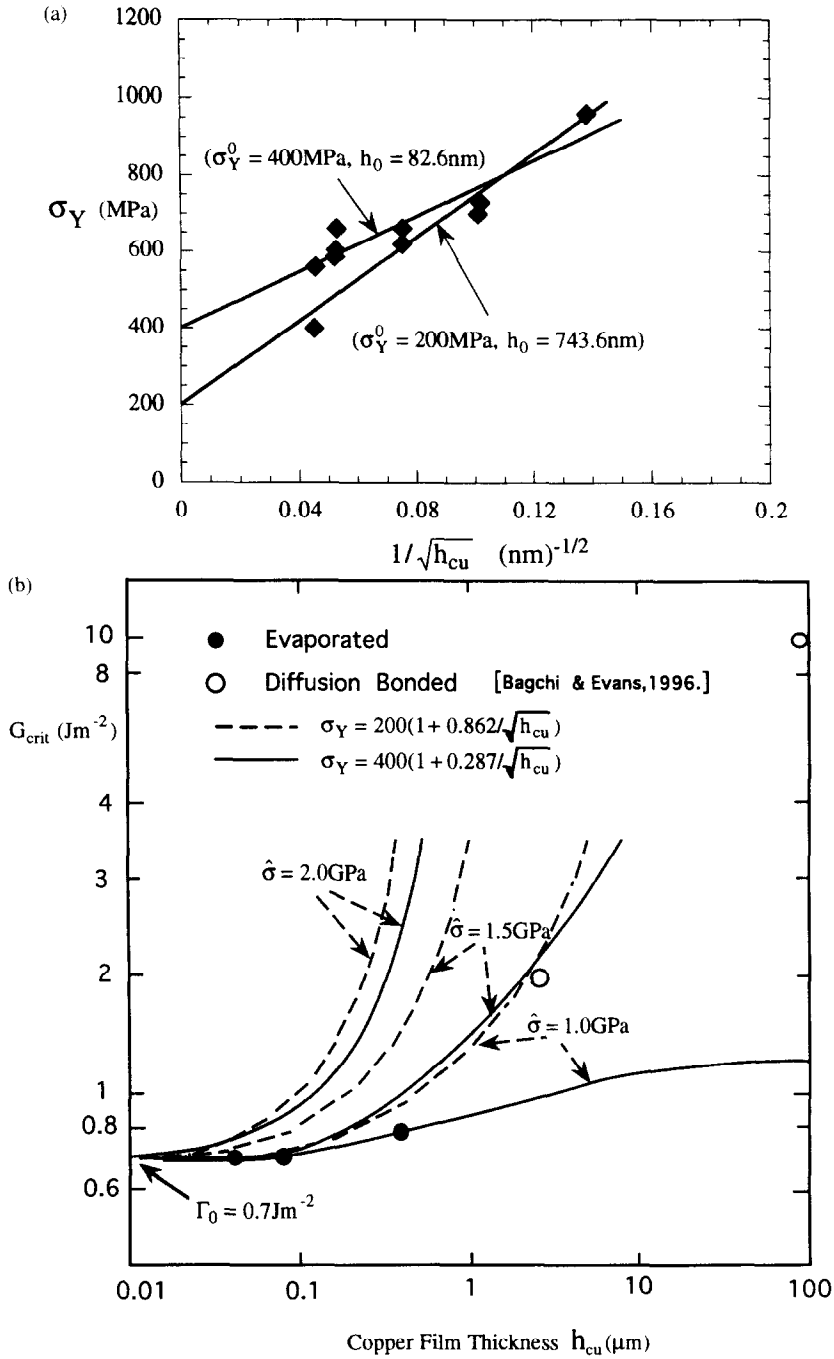

Fig. 12. Application of EPZ model to copper films bonded to silica substrates where the film stress is at yield prior to delamination. (a) Data for thickness dependence of yield stress of copper and two approximations (5.1) to the data. (b) Experimental data for thickness dependence of G_{crit} and comparison with theory for three choices of the peak stress governing interface separation.

yield when delamination occurs, the all-important ratio, $\hat{\sigma}/\sigma_Y$, increases as h_{cu} increases due to the thickness dependence of the copper yield stress. it is this effect which produces the sharp increases in G_{crit} with increasing copper film thickness in this application.

Comparison of the theoretical curves with the experimental data points in Fig. 12(b) suggest that the best fit is obtained with $\hat{\sigma} = 1.5$ GPa if $\sigma_Y^0 = 400$ MPa or with $\hat{\sigma} = 1$ GPa if $\sigma_Y^0 = 200$ MPa. Peak interface separation stresses on the range from 1 to 2 GPa are lower than expected for strong interfaces. However, they may not be unreasonable for the Cu/SiO_2 interface for the following two reasons (A. G. Evans, private communication). The amorphous nature of the SiO_2 is expected to lower somewhat the peak interface separation stress relative to a crystalline substrate. Secondly, carbon has been identified at the interface and its effect as a segregant has been shown in other instances to significantly lower the interface separation stress (Gaudette *et al.*, 1996; Lipkin, 1996).

The model does replicate the main features of the experimental trend seen in Fig. 12(b): an effective interface toughness G_{crit} of very thin films which is nominally the work of the fracture process, increasing to levels that can be many times larger owing to plastic dissipation in the film. It is evident from Fig. 9(a) that the EPZ model as it stands cannot be applied to systems with strong interfaces where the ratio of peak interface separation stress to yield stress, $\hat{\sigma}/\sigma_Y$, is larger than 3 or 4. Conventional plasticity theory, which is employed in carrying out the calculations reported here, predicts interface stresses that are no larger than about 3 or 4 times σ_Y, depending on N. There is a growing body of evidence indicating that conventional plasticity fails to account for flow stress elevation when strain gradients occur at small scales (Fleck and Hutchinson, 1997). Incorporation of plastic strain gradient effects into the EPZ model should result in significantly higher stress levels on the interface in the fracture process zone, thereby permitting the model to be extended to systems with stronger interfaces. As discussed in Section 2.2, the SSV model was proposed, in part, to circumvent the problem associated with the low near-tip stresses. It is expected, however, that applicability of the SSV model will also be limited to weak interfaces unless a more accurate plasticity model is employed to characterize behavior outside the elastic strip. For strong interfaces, the thickness t of the elastic strip must be chosen to be a small fraction of a micron. It is unlikely that conventional plasticity holds down to that scale, and therefore the SSV model appears to share the same limitation as the EPZ model.

ACKNOWLEDGEMENTS

This work was supported in part by the National Science Foundation from Grants MSS-92-02114 and DMR-94-00396 and in part by the Division of Engineering and Applied Sciences at Harvard University.

REFERENCES

Bagchi, A. and Evans, A. G. (1996) The mechanics and physics of thin film decohesion and its measurement. *Interface Sci.* **3**, 169–193.

Bagchi, A., Lucas, G. E., Suo, Z. and Evans, A. G. (1994) A new procedure for measuring the decohesion energy of thin ductile films on substrates. *J. Mater. Res.* **9,** 1734–1741.
Beltz, G. E., Rice, J. R., Shih, C. F. and Xia, L. (1996) A self-consistent model for cleavage in the presence of plastic flow. *Acta Metall. Mater.* **44,** 3943–3954.
Dean, R. H. and Hutchinson, J. W. (1980) Quasi-static steady crack growth in small scale yielding. In *Fracture Mechanics*, ASTM STP 700. pp. 383–405. American Society for Testing Materials, Philadelphia.
Fleck, N. A. and Hutchinson, J. W. (1997) Strain gradient plasticity. *Advances in Applied Mechanics*, ed. J. W. Hutchinson and T. Y. Wu. Vol. 33, pp. 295–361. Academic Press, New York.
Gaudette, F., Suresh, S. and Evans, A. G. (1996) The role of Cr in the debond toughness of γNi/αAl_2O_3 interfaces.
Hutchinson, J. W. (1974) On steady quasi-static crack growth. Harvard University Report DEAP S-8 (AFSOR-TR-74-1042).
Hutchinson, J. W. and Suo, Z. (1992) Mixed mode cracking in layered materials. *Advances in Applied Mechanics*, ed. J. W. Hutchinson and T. W. Wu, Vol. 29, pp. 63–191.
Lipkin, D. (1996) Ph.D. thesis, University of California, Santa Barbara.
Needleman, A. (1987) A continuum model for void nucleation by inclusion debonding. *J. Appl. Mech.* **54,** 525–531.
Nix, W. D. (1989) Mechanical properties of thin films. *Metall. Trans.* **20A,** 2217–2245.
Tvergaard, V. and Hutchinson, J. W. (1992) The relation between crack growth resistance and fracture process parameters in elastic–plastic solids. *J. Mech. Phys. Solids* **40,** 1377–1397.
Tvergaard, V. and Hutchinson, J. W. (1993) The influence of plasticity on mixed mode interface toughness. *J. Mech. Phys. Solids* **41,** 1119–1135.
Tvergaard, V. and Hutchinson, J. W. (1994) Toughness of an interface along a thin ductile layer joining elastic solids. *Phil. Mag.* **A70,** 641–656.
Suo, Z., Shih, C. F. and Varias, A. G. (1993) A theory for cleavage cracking in the presence of plastic flow. *Acta Metall. Mater.* **41,** 151–157.
Vinci, R. P., Zielinski, E. M. and Bravman, J. C. (1995) Thermal strain and stress in copper thin films. *Thin Solid Films* **262,** 142–153.

APPENDIX: STEADY-STATE WORK BALANCE

Work balance relations leading to relation (1.2) are obtained in this Appendix with the aid of a path-independent integral for steady-state crack propagation introduced by Hutchinson (1974). Without additional complication the delamination problem can be generalized to a multilayer whose individual layers have properties that are x_1-independent; both the film and substrate may be layered. A semi-infinite crack advances under steady-state conditions along an interface coinciding with the x_1 axis as depicted in Fig. 13. Plane strain deformations are considered, and the depth of the substrate below the interface is considered to be infinite. Far upstream from the current crack tip the non-zero residual stress component σ_{11} (along with σ_{33}) must be independent of x_1, but may have a general dependence on x_2, i.e. $\sigma_{11} = \sigma_R(x_2)$. Far downstream, the detached film lying above the x_1 axis is unconstrained with zero net force and moment. The possibility of a plastic wake is allowed in both the film and substrate, and the depth of the wake below the interface is denoted by H_P. The results derived below apply to either the embedded process zone model (EPZ model) or the Suo, Shih and Varias (1993) model (SSV model) when conditions for steady-state crack advance are met as prescribed in the body of the paper.

We begin by defining the J-integral and proving its path independence in the context of the film problem just stated. Strains of any material point (x_1, x_2) are measured from the upstream state at (∞, x_2) where the strains (but not the stresses) are taken to be zero. In steady state, a material point at (x_1, x_2) experiences a history that is identical to that of the cumulative history of a spatial sequence of points on the straight line parallel to the interface and connecting to

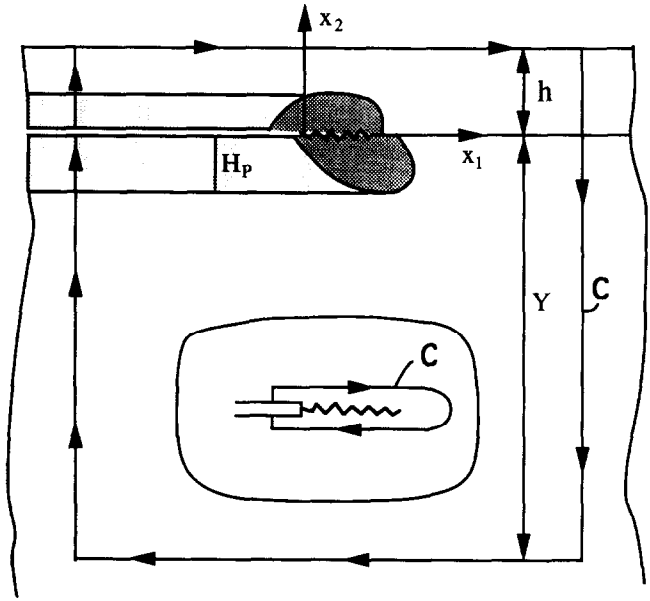

Fig. 13. Conventions for work balance analysis.

(∞, x_2). Let W be the history-dependent work density W of the material point at (x_1, x_2) relative to its initial state at $\varepsilon = 0$. For a steady-state solution,

$$W = \int_0^{\varepsilon} \sigma_{ij}\, \mathrm{d}\varepsilon_{ij} = -\int_{x_1}^{\infty} \sigma_{ij} \frac{\partial \varepsilon_{ij}}{\partial x_1}\, \mathrm{d}x_1. \tag{A.1}$$

Define the line integral I by

$$I = \int_c [W n_1 - \sigma_{ij} n_j u_{i,1}]\, \mathrm{d}s. \tag{A.2}$$

Path independence of I is easily verified. It relies on the expression for W in (A.1) which provides $\partial W/\partial x_1 = \sigma_{ij}\partial \varepsilon_{ij}/\partial x_1$. Thus, for any closed contour c containing no singularities, path independence follows directly from

$$\int_c W n_1\, \mathrm{d}s = \iint_A W_{,1}\, \mathrm{d}A = \iint_A \sigma_{ij}\varepsilon_{ij,1}\, \mathrm{d}A = \iint_A (\sigma_{ij}u_{i,1})_{,j}\, \mathrm{d}A = \int_c \sigma_{ij} n_j u_{i,1}\, \mathrm{d}s. \tag{A.3}$$

Discontinuous material properties across planes parallel to the x_1 axis are permissible as long as they are independent of x_1, which is essential if a steady state is to exist. For a small strain, nonlinear elastic solid (i.e. a deformation theory solid), I is identical to the J-integral. However, no constitutive assumption is involved in either the definition of I or in the proof of its path independence. Path independence is solely a consequence of equilibrium, compatibility, and steady-state conditions. There are no restrictions on the nature on the plastic constitutive relation other than it be time-independent; in particular, non-proportional plastic loading and elastic unloading are fully encompassed.

To apply I to the steady-state film delamination problem, choose a contour C encircling the crack in the sense shown in Fig. 13. By virtue of its path independence, the contour can be shrunk down to the fracture process zone (see insert in Fig. 13) with the result

$$I = \Gamma_0. \tag{A.4}$$

This is obvious for the SSV model because I is necessarily G_{tip} for a crack tip in an elastic region, which, in turn, is required to be Γ_0 for crack advance. For the EPZ model, the shrunken contour shown in the insert in Fig. 13 gives

$$I = -\int_{-d}^{0} T_i[u_{i,1}(x_1, 0^+) - u_{i,1}(x_1, 0^-)]\,dx_1 = -\int_{-d}^{0} T_i \delta_{i,1}\,dx_1 - \int_{0}^{(\delta_n^c, \delta_t^c)} T_i\,d\delta_i = \Gamma_0. \quad (A.5)$$

Next, deform the contour such that it is remote from the tip with vertical segments far upstream as shown in Fig. 13. The contribution to I from the segment of the contour following the upper surface vanishes since the integrand vanishes on a horizontal tracton-free surface. The contribution to I from the horizontal segment along $x_2 = -Y$ deep in the substrate also vanishes as $Y \to \infty$. (The remote stresses and strains in the substrate are on the order of $1/r$ for large r, where r is the distance from the origin.) The contribution to I from the vertical segment far upstream also vanishes since W and $\mathbf{u}$ are defined to vanish far upstream. Only the vertical segment of C far downstream makes a contribution to I, with the result

$$I = \int_{-\infty}^{h} [-W + \sigma_{11}\varepsilon_{11} + \sigma_{12}u_{2,1}]\,dx_2, \quad (A.6)$$

where the integrand is to be evaluated at a value of x_1 far downstream.

To further reduce (A.6), we note that far downstream, W, the strains, and the displacement gradients all vanish below any plastic wake in the substrate. This is a consequence of the fact that an elastic infinitely deep substrate is unperturbed by a layer at its surface, assuming the residual stresses in that layer are independent of x_1. Moreover, σ_{12} vanishes in the remote wake below the interface and in the remote detached film. It follows that (A.6) reduces to

$$I = \int_{-H_p}^{h} [-W + \sigma_{11}\varepsilon_{11}]\,dx_2. \quad (A.7)$$

To simplify the expression further, note that for points far downstream

$$-W + \sigma_{11}\varepsilon_{11} = -\int_0^{\varepsilon} \sigma_{ij}\,d\varepsilon_{ij} + \sigma_{11}\varepsilon_{11} = -[\sigma_{ij}\varepsilon_{ij}]_0^{\varepsilon} + \int_{\sigma_R}^{\sigma} \varepsilon_{ij}\,d\sigma_{ij} + \sigma_{11}\varepsilon_{11} = \int_{\sigma_R}^{\sigma} \varepsilon_{ij}\,d\sigma_{ij}, \quad (A.8)$$

where the last equality follows from the fact that σ_{12} and σ_{22} vanish far downstream and the strains vanish far upstream. The lower integration limit σ_R denotes the residual stress state far upstream. Thus, with a history-dependent complementary work density W_c defined by

$$W_c = \int_{\sigma_R}^{\sigma} \varepsilon_{ij}\,d\sigma_{ij} = -\int_{x_1}^{\infty} \varepsilon_{ij} \frac{\partial \sigma_{ij}}{\partial x_1}\,dx_1, \quad (A.9)$$

$$I = \int_{-H_p}^{h} W_c\,dx_2, \quad (A.10)$$

where it is understood that the integration in (A.10) must be performed on a vertical contour segment far downstream. The most general form of the desired work balance for steady-state delamination is obtained by combining (A.4) and (A.10):

$$\int_{-H_p}^{h} W_c\,dx_2 = \Gamma_0. \quad (A.11)$$

Before reducing (A.11) further, it is useful to specialize it to the limit when no plastic deformation occurs. Denote the non-zero stress component far downstream in the film by $\sigma_{11} = \sigma_D(x_2)$. (In general, σ_{33} will also be non-zero, but it has no influence on the result being sought.) The resultant force and moment due to σ_D must vanish. Any residual stress far

downstream in the substrate will be unchanged from its upstream value when no plasticity occurs in the substrate. Thus, for purely elastic deformations, (A.11) becomes

$$G \equiv \int_0^h \frac{1-\nu^2}{2E}(\sigma_D - \sigma_R)^2 \, dx_2 = \Gamma_0. \tag{A.12}$$

This result is also applicable to a multilayered film whose elastic properties change from layer to layer.†

Consider the case of *an elastic film on an elastic–plastic substrate*. The contribution to the left-hand side of (A.11) from the film is precisely G as defined in (A.12), because the downstream stress distribution $\sigma_D(x_2)$ in the film does not depend on the plastic deformation in the substrate. Consequently, (A.11) can be rewritten with separate film and substrate contributions according to

$$G + \int_{-H_P}^0 W_c \, dx_2 = \Gamma_0. \tag{A.13}$$

Integration by parts in (A.9) for W_c gives

$$W_c = [\varepsilon_{ij}\sigma_{ij}]_{\sigma_R}^{\sigma} - \int_0^{\varepsilon_D} \sigma_{ij} \, d\varepsilon_{ij}. \tag{A.14}$$

Because the strains vanish far upstream and because σ_{22}, σ_{12}, and ε_{11} vanish far downstream in the substrate, it follows that the first terms on the right-hand side of this equation vanish. Now the energy balance (A.13) can be written in the final form (1.2) where the dissipation term due to plasticity is

$$\Gamma_P = \int_{-H_P}^0 \left[\int_0^{\varepsilon_D} \sigma_{ij} \, d\varepsilon_{ij} \right] dx_2. \tag{A.15}$$

The notation ε_D in the upper integration limit of the inner integral is used to emphasize that the integral represents the work done on a material element which starts far upstream and ends up far downstream. If no plastic deformation occurs in the substrate, the stresses and strains far upstream and downstream in the substrate are identical and Γ_P is zero. When plastic deformation occurs, the dissipation term includes both the plastic deformation work and an elastic work contribution since, in general, the downstream stresses will no longer equal the upstream stresses in the wake.

Lastly, consider the case of an *elastic–plastic film on an elastic substrate*. Now only the film contributes to (A.11). Separate the strains into elastic and plastic parts such that W_c becomes

$$W_c = \int_{\sigma_R}^{\sigma_D} \varepsilon_{ij}^e \, d\sigma_{ij} + \int_{\sigma_R}^{\sigma_D} \varepsilon_{ij}^P \, d\sigma_{ij}. \tag{A.16}$$

the first term is

$$\int_{\sigma_R}^{\sigma_D} \varepsilon_{ij}^e \, d\sigma_{ij} = ((1-\nu^2)/(2E))(\sigma_D - \sigma_R)^2,$$

but in this case the downstream stress distribution σ_D depends on the plastic deformation occurring in the film. Define G^* to be the elastic energy release rate *computed using the actual downstream stress distribution* σ_D:

† It is readily shown that an alternative expression for G is $\int_0^h [(1-\nu^2)/2]E(\sigma_D^2 - \sigma_R^2) \, dx_2$.

$$G^* = \int_0^h \frac{(1-\nu^2)}{2E}(\sigma_D - \sigma_R)^2 \, dx_2. \tag{A.17}$$

The energy balance equation (A.11) now becomes

$$G^* = \Gamma_0 - \int_0^h \left[\int_{\sigma_R}^{\sigma_D} \varepsilon_{ij}^P \, d\sigma_{ij} \right] dx_2. \tag{A.18}$$

Finally, it is useful to put this equation into the form (1.2). To this end, let G be the elastic energy release rate *defined using the downstream stress distribution* σ_D *computed as if no plastic deformation occurred in the film*. That is, define G as the right-hand side of (A.17), where σ_D is computed on the basis of an elastic analysis. (This is how G is defined for the elastic–plastic film in the body of this paper.) With this definition, (1.2) holds where

$$\Gamma_P = G - G^* - \int_0^h \left[\int_{\sigma_R}^{\sigma_D} \varepsilon_{ij}^P \, d\sigma_{ij} \right] dx_2. \tag{A.19}$$